On Physical Layer Security of α-η-κ-μ Fading Channels

Aashish Mathur, *Member, IEEE*, Yun Ai, *Member, IEEE*, Manav R. Bhatnagar, *Senior Member, IEEE*, Michael Cheffena, and Tomoaki Ohtsuki, *Senior Member, IEEE*

***Abstract*—In this letter, we study the secrecy performance of the classic Wyner's wiretap model, where the main and eavesdropper channels are modeled by a general and versatile α-η-κ-μ fading model. Novel and exact expressions of the average secrecy capacity and secrecy outage probability have been derived. Previous results on physical layer security can be obtained through our newly derived expressions by specializing the model parameters. More importantly, the derived results are also applicable for the secrecy performance analysis of some field measurements (e.g. in millimeter wave communications), which cannot be analyzed by previous results.**

***Index Terms*—Physical layer security, secrecy capacity, secrecy outage probability, generalized fading, short-term fading.**

I. Introduction

PHYSICAL LAYER SECURITY (PLS) has been considered as a potential paradigm to enhance communication secrecy against eavesdropping in wireless communication networks [1]. The physical layer secrecy performance of communication systems over different short-term fading conditions such as Rayleigh, Hoyt, Rice, Weibull, κ-μ, and α-μ, etc., has been explored in [2]–[5] and the references therein. On the other hand, the emerging wireless applications and services expand the traditional outdoor channel environments to all sorts of new scenarios such as millimeter wave (mm-Wave) communications, body area networks, vehicle-to-everything, Internet of Things, etc [6]. It is found in recent studies that in some of these emerging communication scenarios (e.g. mobile-to-mobile communications and indoor-to-outdoor propagation in fifth generation (5G) networks), none of the aforementioned traditional and well-established fading distributions follows the experimental data satisfactorily [7]–[9]. This necessitates the establishment of a general and versatile channel model to adapt different fading behaviors resulting from the new propagation scenarios.

Recently, a new fading distribution called α-η-κ-μ distribution has been proposed in [9], which is probably the most comprehensive and unifying fading model in open literature as it encompasses the most traditional and well-established models such as Rayleigh, Rice, Hoyt, Weibull, α-μ, and κ-μ distributions as its special cases [9], [10]. This model is developed on a physical basis, where the parameters correctly describe the short-term propagation phenomena such as nonlinearity of the propagation medium, number of multipath clusters, and powers of the dominant and diffused components. The model is very useful for accurate modeling of the scenarios, where the conventional models may not correctly hold [7]–[9], [11]. For instance, extensive channel measurement campaigns at 28 GHz in outdoor line-of-sight (LOS) and non-LOS (NLOS) conditions and at 60 GHz in LOS conditions for mm-Wave communications were conducted in [11], and it was found that the α-η-κ-μ model best fits the experimental data. Further, the non-unimodal nature of the α-η-κ-μ envelope makes it a potentially suitable channel model for device-to-device communications, mobile-to-mobile communications, vehicle-to-vehicle communications, indoor-to-outdoor propagation in 5G, military high-frequency (HF) communications, millimeter communications, and ionospheric scintillation [9].

To the best of the authors' knowledge, the secrecy performance of communication systems over this comprehensive fading model is still unexplored. This motivates us to conduct the secrecy performance analysis of communication systems over the α-η-κ-μ fading channels. The main contributions of this letter are as follows:

1) A novel series based expression for the average secrecy capacity (ASC) is derived in terms of the extended generalized bivariate Fox H function (EGBFHF) for the classical Wyner's model [12] under the α-η-κ-μ fading.
2) Exact and generalized expression is obtained for the secrecy outage probability (SOP) in terms of the Meijer G function contrary to previous works [2], [13], [14], where only lower bound of SOP is derived. The strictly positive secrecy capacity (SPSC) can be obtained from the derived SOP by setting the target secrecy rate to zero.
3) Some useful insights into the system are also provided through the asymptotic ASC analysis and the diversity analysis based on the exact expression of the SOP.
4) The derived results enable to evaluate the impacts of physical channel phenomena such as channel nonlinearity, scattering, and multipath clustering, etc., on the secrecy performance.

The obtained analytical expressions are instrumental in studying the secrecy performance over generalized fading scenarios that are not necessarily restricted to the traditional fading conditions.

II. Channel and System Models

A. The α-η-κ-μ Channel Model: Preliminaries

The envelope probability density function (PDF) of the α-η-κ-μ fading [9] is given by

$$f_R(\rho) = \frac{\alpha \rho^{\alpha\mu-1} e^{-\left(\frac{\rho^\alpha}{2}\right)}}{2^\mu \Gamma(\mu)} \sum_{k=0}^{\infty} \frac{k! c_k}{(\mu)_k} L_k^{\mu-1}(2\rho^\alpha), \qquad (1)$$

Manuscript received MONTH DAY, 2018; revised MONTH DAY, 2018; accepted MONTH DAY, 2018. Date of publication MONTH DAY, 2018; date of current version MONTH DAY, 2018. The associate editor coordinating the review of this paper and approving it for publication was A. El Shafie. *(Corresponding author: Yun Ai.)*

A. Mathur is with the Department of Electrical Engineering, Indian Institute of Technology Jodhpur, Jodhpur, 342037, India (e-mail: aashishmathur@iitj.ac.in).

Y. Ai and M. Cheffena are with the Faculty of Engineering, Norwegian University of Science and Technology, 2815 Gjøvik, Norway (e-mails: yun.ai@ntnu.no; michael.cheffena@ntnu.no).

M. R. Bhatnagar is with the Department of Electrical Engineering, Indian Institute of Technology - Delhi, Hauz Khas, New Delhi 110016, India (e-mail: manav@ee.iitd.ac.in).

T. Ohtsuki is with the Department of Information and Computer Science, Keio University, Yokohama 223-8522, Japan (e-mail: ohtsuki@ics.keio.ac.jp).

Digital Object Identifier

$$I_1 = \frac{2^{-(\mu_B+\mu_E+2)}\alpha_B \overline{\gamma_B}^{\frac{-\alpha_B\mu_B}{2}}}{\Gamma(\mu_B)\Gamma(\mu_E+1)\overline{\gamma_E}^{\frac{\alpha_E\mu_E}{2}}} \sum_{k=0}^{\infty} \frac{k! c_{k,B}}{(\mu_B)_k} \sum_{n=0}^{\infty} \frac{n! m_{n,E}}{(\mu_E+1)_n} \sum_{r=0}^{k} \frac{(-1)^r 2^r \binom{k+\mu_B-1}{k-r}}{r! \overline{\gamma_B}^{\frac{\alpha_B r}{2}}} \sum_{s=0}^{n} \frac{(-1)^s 2^s (\mu_E+1)^s \binom{n+\mu_E}{n-s}}{s! \mu_E^s \overline{\gamma_E}^{\frac{\alpha_E s}{2}}}$$
$$\times (2\overline{\gamma_B}^{\frac{\alpha_B}{2}})^{\frac{\alpha_E(\mu_E+s)}{\alpha_B}+\mu_B+r} H_{1,0:0,1:2,2}^{0,1:1,0:1,2} \left(\begin{matrix} (1-(\mu_B+r+\frac{\alpha_E(\mu_E+s)}{\alpha_B}); \frac{\alpha_E}{\alpha_B}, \frac{2}{\alpha_B}) \\ - \end{matrix} \middle| \begin{matrix} - \\ (0,1) \end{matrix} \middle| \begin{matrix} (1,1),(1,1) \\ (1,1),(0,1) \end{matrix} \middle| \begin{matrix} \frac{(2\overline{\gamma_B}^{\frac{\alpha_B}{2}})^{\frac{\alpha_E}{\alpha_B}}}{2\overline{\gamma_E}^{\frac{\alpha_E}{2}}}, 2^{\frac{2}{\alpha_B}} \overline{\gamma_B} \end{matrix} \right) \quad (8)$$

where $L_n^m(\cdot)$ is the Laguerre polynomial [15, Eq. (8.970.1)], $(\cdot)_n$ is the Pochhammer symbol [16, Eq. (6.1.22)], and $\Gamma(\cdot)$ is the Gamma function [15, Eq. (8.310.1)]. The PDF in (1) is described by the positive parameters α, η, κ, μ, p, and q, where α is the non-linearity parameter of the channel, η gives the ratio of the total power of the in-phase and quadrature scattered waves of the multipath clusters, κ signifies the total power of the dominant components divided by the total power of scattered waves, μ represents the total number of multipath clusters, p is the ratio of the number of multipath clusters of the in-phase and quadrature signals, and q is defined as the ratio of two ratios: the ratio of the power of the dominant components to the power of the scattered waves of the in-phase signal and its counterpart for the quadrature signal. The parameter c_k in (1) is computed with the aid of parameters α, η, κ, μ, p, and q using the recursive relation in [9, Eq. (15)] and the relations given by [9, Eqs. (30) and (31)].

The cumulative distribution function (CDF) of the envelope of α-η-κ-μ fading model is given by [9]

$$F_R(\rho) = \frac{\rho^{\alpha\mu} e^{-\left(\frac{\rho^\alpha}{2}\right)}}{2^{\mu+1}\Gamma(\mu+1)} \sum_{k=0}^{\infty} \frac{k! m_k}{(\mu+1)_k} L_k^{\mu}\Big(\frac{2(\mu+1)\rho^\alpha}{\mu}\Big). \quad (2)$$

In (2), m_k is obtained with the help of the parameters α, η, κ, μ, p, and q using the recursive relation in [9, Eq. 16] and the expressions given by [9, Eqs. (33) and (34)].

B. System Model

In this letter, we consider the classic Wyner's wiretap model [12] for our analysis, where the legitimate transmitter, Alice (node A), transmits confidential information signal to the legitimate receiver, Bob (node B), over the main channel. The eavesdropper, Eve (node E), tries to intercept these messages by decoding its received signal through the eavesdropper channel. It is assumed that the main and eavesdropper channels experience independent but not necessarily identical α-η-κ-μ fading and the channel coefficients remain constant during the transmission of a block of codewords.

The instantaneous signal-to-noise-ratio (SNR) at node X, $X \in \{B, E\}$, is expressed as

$$\gamma_X = \frac{R_X^2 E_s}{N_{0,X}} = R_X^2 \overline{\gamma_X}, \quad (3)$$

where R_X represents the received signal envelope at node X, E_s is the transmitted signal energy, $N_{0,X}$ is the power spectral density of the additive white Gaussian noise (AWGN) on the corresponding links, and $\overline{\gamma_X} = E_s/N_{0,X}$. Using (1) and (3), the PDF of the instantaneous SNR at node X is given as follows:

$$f_{\gamma_X}(\gamma) = \frac{\alpha_X \gamma^{\frac{\alpha_X\mu_X}{2}-1}}{2^{\mu_X+1}\Gamma(\mu_X)\overline{\gamma_X}^{\frac{\alpha_X\mu_X}{2}}} \exp\Big(\frac{-\gamma^{\frac{\alpha_X}{2}}}{2\overline{\gamma_X}^{\frac{\alpha_X}{2}}}\Big) \times \sum_{k=0}^{\infty} \frac{k! c_{k,X}}{(\mu_X)_k} L_k^{\mu_X-1}\Big(2\Big(\frac{\gamma}{\overline{\gamma_X}}\Big)^{\frac{\alpha_X}{2}}\Big). \quad (4)$$

Similarly, the CDF of the instantaneous SNR at node X is given by

$$F_{\gamma_X}(\gamma) = \frac{\left(\frac{\gamma}{\overline{\gamma_X}}\right)^{\frac{\alpha_X\mu_X}{2}} \exp\left(\frac{-\gamma^{\frac{\alpha_X}{2}}}{2\overline{\gamma_X}^{\frac{\alpha_X}{2}}}\right)}{2^{\mu_X+1}\Gamma(\mu_X+1)} \sum_{k=0}^{\infty} \frac{k! m_{k,X}}{(\mu_X+1)_k} \times L_k^{\mu_X}\Big(\frac{2(\mu_X+1)}{\mu_X}\Big(\frac{\gamma}{\overline{\gamma_X}}\Big)^{\frac{\alpha_X}{2}}\Big). \quad (5)$$

III. Secrecy Performance Analysis

A. ASC Analysis

In the scenario of active eavesdropping, full channel state information (CSI) of both the main and eavesdropper channels is available to the node A, which can adapt the achievable secrecy rate accordingly. In this case, the instantaneous secrecy capacity of the considered system is defined as $C_s(\gamma_B, \gamma_E) = \max\{\ln(1+\gamma_B) - \ln(1+\gamma_E), 0\}$ [2]. The ASC, $\overline{C}_s$, can be obtained from [2]

$$\begin{aligned} \overline{C}_s &= \mathbb{E}\{C_s(\gamma_B, \gamma_E)\} \\ &= \int_0^\infty \int_0^\infty C_s(\gamma_B, \gamma_E) f_{\gamma_B,\gamma_E}(\gamma_B, \gamma_E)\, d\gamma_B d\gamma_E \\ &= I_1 + I_2 - I_3, \end{aligned} \quad (6)$$

where $f_{\gamma_B,\gamma_E}(\gamma_B, \gamma_E) = f_{\gamma_B}(\gamma_B) f_{\gamma_E}(\gamma_E)$ due to the independence of the two links, and $I_1 = \int_0^\infty \ln(1+\gamma_B) f_{\gamma_B}(\gamma_B) F_{\gamma_E}(\gamma_B)\, d\gamma_B$, $I_2 = \int_0^\infty \ln(1+\gamma_E) f_{\gamma_E}(\gamma_E) F_{\gamma_B}(\gamma_E)\, d\gamma_E$, and $I_3 = \int_0^\infty \ln(1+\gamma_E) f_{\gamma_E}(\gamma_E)\, d\gamma_E$.

On substituting the PDF of γ_B and the CDF of γ_E from (4) and (5), respectively, into I_1, and using [15, Eq. 8.970.1], the integral in I_1 can be re-written by expressing the $\ln(\cdot)$ and $\exp(\cdot)$ functions in their corresponding Meijer G representation using [17, Eq. (8.4.6.4)] and [17, Eq. (8.4.3.1)], respectively, and then utilizing [18, Eq. (6.2.8)] to get

$$I_1 = \frac{2^{-(\mu_B+\mu_E+2)}\alpha_B}{\Gamma(\mu_B)\Gamma(\mu_E+1)\overline{\gamma_B}^{\frac{\alpha_B\mu_B}{2}}\overline{\gamma_E}^{\frac{\alpha_E\mu_E}{2}}} \sum_{k=0}^{\infty} \frac{k! c_{k,B}}{(\mu_B)_k} \times \sum_{n=0}^{\infty} \frac{n! m_{n,E}}{(\mu_E+1)_n} \sum_{r=0}^{k} \frac{(-1)^r 2^r}{r! \overline{\gamma_B}^{\frac{\alpha_B r}{2}}} \binom{k+\mu_B-1}{k-r} \sum_{s=0}^{n} \frac{(-1)^s}{s!} \times \frac{2^s(\mu_E+1)^s}{\mu_E^s \overline{\gamma_E}^{\frac{\alpha_E s}{2}}} \binom{n+\mu_E}{n-s} \int_0^\infty \gamma_B^{\frac{\alpha_B\mu_B}{2}+\frac{\alpha_E\mu_E}{2}+\frac{\alpha_B r}{2}+\frac{\alpha_E s}{2}-1} \times H_{0,1}^{1,0}\left(\frac{\gamma_B^{\frac{\alpha_B}{2}}}{2\overline{\gamma_B}^{\frac{\alpha_B}{2}}} \middle| \begin{matrix} - \\ (0,1) \end{matrix}\right) H_{0,1}^{1,0}\left(\frac{\gamma_B^{\frac{\alpha_E}{2}}}{2\overline{\gamma_E}^{\frac{\alpha_E}{2}}} \middle| \begin{matrix} - \\ (0,1) \end{matrix}\right) \times H_{2,2}^{1,2}\left(\gamma_B \middle| \begin{matrix} (1,1),(1,1) \\ (1,1),(0,1) \end{matrix}\right) d\gamma_B. \quad (7)$$

In (7), $H_{p,q}^{m,n}(\cdot|:)$ is the Fox H function [17, Eq. (8.3.1)]. The integral in (7) can be solved with the help of [19, Eq. (2.3)] and is expressed in terms of the EGBFHF, $H_{p,q:t,u:w,x}^{m,n:r,s:v,u}(\cdot)$, given by (8) at the top of this page. The EGBFHF function can be implemented in Mathematica [12].

$$P_o = \frac{2^{-(\mu_E+\mu_B+\alpha_E+1)}\overline{\gamma_B}^{\frac{-\alpha_B\mu_B}{2}}}{\pi^{\alpha_E-\frac{1}{2}}\Gamma(\mu_E)\Gamma(\mu_B)\overline{\gamma_E}^{\frac{\alpha_E\mu_E}{2}}}\sum_{n=0}^{\infty}\frac{n!c_{n,E}}{(\mu_E)_n}\sum_{s=0}^{n}\frac{(-1)^s 2^s\binom{n+\mu_E-1}{n-s}}{s!\overline{\gamma_E}^{\frac{\alpha_E s}{2}}\left(\frac{\Theta}{\Theta-1}\right)^{\frac{\alpha_E(\mu_E+s)}{2}}}\sum_{k=0}^{\infty}\frac{k!c_{k,B}}{(\mu_B)_k}\sum_{r=0}^{k}\frac{(-1)^r 2^{r+1}\binom{k+\mu_B-1}{k-r}}{r!\overline{\gamma_B}^{\frac{\alpha_B r}{2}}}$$
$$\times\sum_{l=0}^{\infty}\frac{(-1)^l(2\overline{\gamma_B}^{\frac{\alpha_B}{2}})^{-l}\left(\frac{\Theta-1}{\alpha_E}\right)^{\frac{\alpha_B(\mu_B+r+l)}{2}}}{l!(\mu_B+r+l)\Gamma(\frac{-\alpha_B(\mu_B+r+l)}{2})}G_{\alpha_E,2+\alpha_E}^{2+\alpha_E,\alpha_E}\left(\frac{1}{16}\left(\frac{\Theta-1}{\Theta\overline{\gamma_E}}\right)^{\alpha_E}\middle|\begin{matrix}\Delta\left(\alpha_E,1-\frac{\alpha_E(\mu_E+s)}{2}\right)\\ \Delta(2,0),\Delta\left(\alpha_E,-\frac{\alpha_E(\mu_E+s)}{2}-\frac{\alpha_B(\mu_B+r+l)}{2}\right)\end{matrix}\right). \quad (15)$$

Similarly, I_2 can be obtained by replacing α_B, μ_B, and $\overline{\gamma_B}$ in (8) with α_E, μ_E, and $\overline{\gamma_E}$ and vice-versa. For computing I_3, we substitute (4) into the expression of I_3. By using [15, Eq. (8.970.1)] and [17, Eqs. (8.4.6.5) and (8.4.3.1)], the integral in I_3 is converted to a form similar to [17, Eq. (2.24.1.1)]. After some manipulations, the following simplified form for I_3 is obtained:

$$I_3 = \sum_{k=0}^{\infty}\sum_{l=0}^{k}\frac{(-1)^l 2^{l-\mu_E-\frac{1}{2}}k!c_{k,E}\binom{k+\mu_E-1}{k-l}}{(2\pi)^{\alpha_E-\frac{1}{2}}l!\Gamma(\mu_E)(\mu_E)_k\overline{\gamma_E}^{\frac{\alpha_E(\mu_E+l)}{2}}} \times G_{2\alpha_E,2+2\alpha_E}^{2+2\alpha_E,2\alpha_E}\left(\frac{1}{16\overline{\gamma_E}^{\alpha_E}}\middle|\begin{matrix}\phi_1,\phi_2\\ \Delta(2,0),\phi_1,\phi_1\end{matrix}\right), \quad (9)$$

where $\phi_1 = \Delta\big(\alpha_E, \frac{-\alpha_E(\mu_E+l)}{2}\big)$, $\phi_2 = \Delta\big(\alpha_E, 1-\frac{\alpha_E(\mu_E+l)}{2}\big)$, and $\Delta(a,b) = \frac{b}{a}, \frac{b+1}{a}, ..., \frac{b+a-1}{a}$. Thus, ASC can be evaluated by putting (8) and (9) into (6).

Remark 1: Although the expressions in (8) and (9) are expressed in terms of infinite series, these infinite summations converge quickly for finitely small values of k and n, which is also justified by the numerical results in Fig. 1. For instance, the ASC for the special case of Rayleigh fading is obtained using $k = 10$ and $n = 10$ in Fig. 1.

B. Asymptotic ASC Analysis

To obtain more insights on the ASC, the asymptotic analysis is conducted for the ASC performance in the high transmit SNR regime, namely assuming $\overline{\gamma_B} = \overline{\gamma_E} = \overline{\gamma} \to \infty$. Using the definition of secrecy capacity [12, Eq. (6)] and applying the transformation $\gamma_B = |R_B|^2\overline{\gamma} = u\overline{\gamma}$ and $\gamma_E = |R_E|^2\overline{\gamma} = v\overline{\gamma}$, the asymptotic ASC is written as

$$\overline{C}_s \approx \frac{\alpha_E\alpha_B}{2^{\mu_E+\mu_B+2}\Gamma(\mu_E)\Gamma(\mu_B)}\sum_{k=0}^{\infty}\frac{k!c_{k,E}}{(\mu_E)_k}\sum_{l=0}^{\infty}\frac{l!c_{l,B}}{(\mu_B)_l} \times (J_1 - J_2), \quad (10)$$

where $J_1 = \int_0^{\infty} v^{\frac{\alpha_E\mu_E}{2}-1}e^{\left(\frac{-v^{\frac{\alpha_E}{2}}}{2}\right)}L_k^{\mu_E-1}(2v^{\frac{\alpha_E}{2}})\int_v^{\infty}\ln(u) \times u^{\frac{\alpha_B\mu_B}{2}-1}e^{\left(\frac{-u^{\frac{\alpha_B}{2}}}{2}\right)}L_l^{\mu_B-1}(2u^{\frac{\alpha_B}{2}})dudv$ and $J_2 = \int_0^{\infty}\ln(v) \times v^{\frac{\alpha_E\mu_E}{2}-1}e^{\left(\frac{-v^{\frac{\alpha_E}{2}}}{2}\right)}L_k^{\mu_E-1}(2v^{\frac{\alpha_E}{2}})\int_v^{\infty}u^{\frac{\alpha_B\mu_B}{2}-1}e^{\left(\frac{-u^{\frac{\alpha_B}{2}}}{2}\right)} \times L_l^{\mu_B-1}(2u^{\frac{\alpha_B}{2}})dudv$. J_1 is evaluated by changing the integration order and using [15, Eqs. (8.970.1) and (3.381.1)] to have

$$J_1 = \frac{8}{\alpha_E\alpha_B}\sum_{r=0}^{k}\frac{(-1)^r 2^{\mu_E+2r}}{r!}\binom{k+\mu_E-1}{k-r}\sum_{i=1}^{N}w_i g_1(x_i), \quad (11)$$

where x_i and w_i are the abscissas and weight factors of the Gauss Laguerre integration [16, Eq. (25.4.45)], $g_1(x) = (2x)^{\mu_B-1}L_l^{\mu_B-1}(4x)\gamma(\mu_E+r, \frac{(2x)^{\frac{\alpha_E}{\alpha_B}}}{2})\ln(2x)^{\frac{2}{\alpha_B}}$, and $\gamma(\cdot,\cdot)$ is the lower incomplete Gamma function. Similarly, J_2 can be solved by using [15, Eqs. (8.970.1) and (3.381.3)] to get

$$J_2 = \frac{8}{\alpha_E\alpha_B}\sum_{s=0}^{l}\frac{(-1)^s 2^{\mu_B+2s}}{s!}\binom{l+\mu_B-1}{l-s}\sum_{i=1}^{N}w_i g_2(x_i). \quad (12)$$

In (12), $g_2(x) = (2x)^{\mu_E-1}L_k^{\mu_E-1}(4x)\Gamma(\mu_B + s, \frac{(2x)^{\frac{\alpha_B}{\alpha_E}}}{2})\ln(2x)^{\frac{2}{\alpha_E}}$ and $\Gamma(\cdot,\cdot)$ is the upper incomplete Gamma function. Employing (11) and (12) into (10), we obtain the expression for the asymptotic ASC.

C. SOP Analysis

The SOP is a useful secrecy performance metric for the passive eavesdropping scenario, where node A does not have CSI on the eavesdropper's channel. The SOP is defined as the probability that the instantaneous secrecy capacity is below a threshold rate R_s [5], i.e.,

$$P_o = \Pr[C_s(\gamma_B,\gamma_E) \le R_s] = \Pr[\gamma_B \le \Theta\gamma_E + \Theta - 1] = \int_0^{\infty} f_{\gamma_E}(\gamma_E)\Big(\int_0^{(1+\gamma_E)\Theta-1} f_{\gamma_B}(\gamma_B)d\gamma_B\Big)d\gamma_E, \quad (13)$$

where $\Theta = \exp(R_s) \ge 1$. Substituting (4) into (13), using the series expansion of the Laguerre polynomial [15, Eq. (8.970.1)], and applying the transformation $\gamma_B^{(\alpha_B/2)} = y$, the inner integral in (13) is solved using [15, Eq. (3.381.1)] to obtain

$$P_o = \frac{\alpha_E 2^{-(\mu_E+\mu_B+2)}\overline{\gamma_B}^{\frac{-\alpha_B\mu_B}{2}}}{\Gamma(\mu_E)\Gamma(\mu_B)\overline{\gamma_E}^{\frac{\alpha_E\mu_E}{2}}}\sum_{n=0}^{\infty}\frac{n!c_{n,E}}{(\mu_E)_n}\sum_{s=0}^{n}\frac{(-1)^s 2^s}{s!\overline{\gamma_E}^{\frac{\alpha_E s}{2}}} \times \binom{n+\mu_E-1}{n-s}\sum_{k=0}^{\infty}\frac{k!c_{k,B}}{(\mu_B)_k}\sum_{r=0}^{k}\frac{(-1)^r 2^{r+1}}{r!\overline{\gamma_B}^{\frac{\alpha_B r}{2}}} \times \binom{k+\mu_B-1}{k-r}(2\overline{\gamma_B}^{\frac{\alpha_B}{2}})^{\mu_B+r}\int_0^{\infty}\gamma_E^{\frac{\alpha_E(\mu_E+s)}{2}-1} \times \exp\left(\frac{-\gamma_E^{\frac{\alpha_E}{2}}}{2\overline{\gamma_E}^{\frac{\alpha_E}{2}}}\right)\gamma\Big(\mu_B+r, \frac{((1+\gamma_E)\Theta-1)^{\frac{\alpha_B}{2}}}{2\overline{\gamma_B}^{\frac{\alpha_B}{2}}}\Big)d\gamma_E. \quad (14)$$

Now, using [15, Eq. (8.354.1)] and [20, Eqs. (10) and (11)], (14) is converted to a form similar to [17, Eq. (2.24.1.1)]. Thus, P_o is given by (15) at the top of the page.

TABLE I
PARAMETER VALUES FOR NUMERICAL RESULTS [9], [11]

Fading	$(\alpha, \eta, \kappa, \mu, p, q)$
$Nakagami-$m	(2, 1, 0, 0.7, 1, 1)
$Hoyt$	(2, 3, 0, 0.5, 1, 1)
$Rayleigh$	(2, 1, 0, 1, 1, 1)
$Weibull$	(3, 1, 0, 1, 1, 1)
60 GHz $(LOS, indoor)$	(3.49, 0.12, 0.6, 0.79, 0.5, 0.07)
28 GHz $(LOS, outdoor)$	(2.2, 73, 5.7, 1.01, 1.05, 1)
28 GHz $(NLOS, outdoor)$	(2.545, 0.006, 2.5, 1.98, 1.5, 1.05)

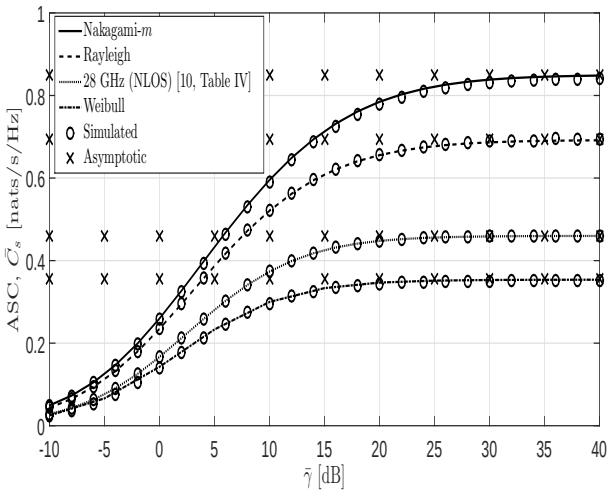

Fig. 1. Comparison of analytical (6), simulated, and asymptotic (10) ASC versus average SNR for various fading scenarios using parameter values from Table I.

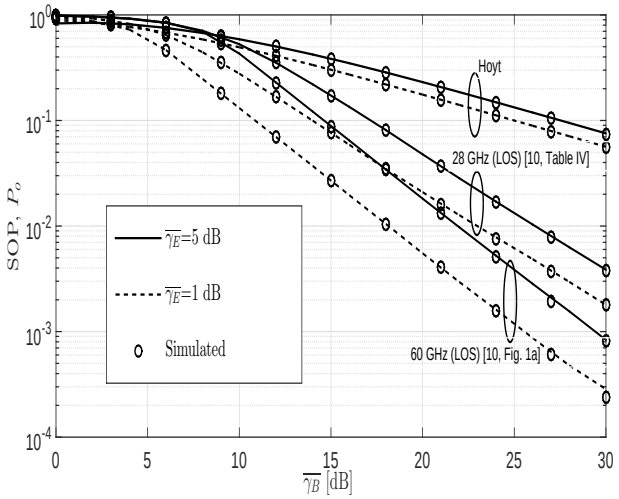

Fig. 2. Comparison of analytical (15) and simulated SOP versus $\overline{\gamma_B}$ for different fading scenarios using parameter values from Table I.

Remark 2: For diversity analysis, we analyze (15) for high values of $\overline{\gamma_B}$ for a fixed $\overline{\gamma_E}$. At high $\overline{\gamma_B}$, the dominant term in (15) would correspond to the smallest exponent of $\overline{\gamma_B}$. Thus, the SOP curves fall with a slope of $\frac{\alpha_B \mu_B}{2}$ at high $\overline{\gamma_B}$ implying that the diversity order based on SOP depends only on the channel non-linearity and the number of multipath clusters.

IV. Numerical Results And Discussions

Assuming $\alpha_B = \alpha_E = \alpha$, $\mu_B = \mu_E = \mu$, $\kappa_B = \kappa_E = \kappa$, and $\eta_B = \eta_E = \eta$, the model parameter values used for the simulation are provided in Table I, where the last three data sets are extracted from the field measurements [11].

Figure 1 shows the comparison of ASC for different fading scenarios, which are obtained as special cases of the α-η-κ-μ fading model. We observe from Fig. 1 that for high transmit SNR, there is no improvement in ASC with the SNR. This is also justified by the asymptotic ASC derived in (10), which is independent of $\overline{\gamma}$. It is also noted that as the value of α increases from 2 to 4 keeping $\mu = 1$, $\kappa = 0$, and $\eta = p$, the ASC deteriorates. Similarly, on reducing μ from 1 to 0.7 for $\alpha = 2$, $\kappa = 0$, and $\eta = p$, the ASC becomes better. As α or μ increases, both the main channel and eavesdropper channel become better and have higher individual capacities, but the resulting capacity difference between these two is small and hence, ASC is small. Similar trends are also observed in [12] for the α-μ fading channel, which is a special case of the α-η-κ-μ channel.

In Fig. 2, we compare the SOP as a function of $\overline{\gamma_B}$ for different values of $\overline{\gamma_E}$ and $R_s = 1$. It is seen from the figure that as the eavesdropper SNR, $\overline{\gamma_E}$, increases, the SOP deteriorates. Moreover, the SOP performance improves in good channel conditions, which corresponds to higher values of the parameters α, η, κ, and μ.

Remark 3: The versatility of the derived results over α-η-κ-μ fading model is clearly depicted through the numerical results. Not only does this model map to the well-known fading scenarios, it also describes generalized fading scenarios, where the traditional models do not fit well.

References

[1] N. Yang *et al.*,"Safeguarding 5G wireless communication networks using physical layer security,"*IEEE Commun. Mag.*, vol. 53, no. 4, pp. 20–27, Apr. 2015.

[2] N. Bhargav *et al.*,"Secrecy capacity analysis over κ-μ fading channels: Theory and applications," *IEEE Trans. Commun.*, vol. 64, no. 7, pp. 3011–3024, Jul. 2016.

[3] J. M. Romero-Jerez and F. J. Lopez-Martinez, "A new framework for the performance analysis of wireless communications under Hoyt (Nakagami-q) fading," *IEEE Trans. Inf. Theory*, vol. 63, no. 3, pp. 1693–1702, Mar. 2017.

[4] F. Jameel *et al.*,"Secrecy outage for wireless sensor networks," *IEEE Commun. Lett.*, vol. 21, no. 7, pp. 1565–1568, Jul. 2017.

[5] H. Lei *et al.*, "Performance analysis of physical layer security over Generalized-K fading channels using a mixture Gamma distribution," *IEEE Commun. Lett.*, vol. 20, no. 2, pp. 408–411, Feb. 2016.

[6] D. Raychaudhuri and M. Gerla, *Emerging Wireless Technologies and the Future Mobile Internet*, Cambridge, U.K.: Cambridge Univ. Press, 2011.

[7] Y. Ibdah and Y. Ding, "Mobile-to-mobile channel measurements at 1.85 GHz in suburban environments," *IEEE Trans. Commun.*, vol. 63, no. 2, pp. 466–475, Feb. 2015.

[8] S. Hamid *et al.*, "Inside-out propagation: Developing a unified model for the interference in 5G networks," *IEEE Veh. Technol. Mag.*, vol. 10, no. 2, pp. 47–54, Jun. 2015.

[9] M. D. Yacoub, "The α-η-κ-μ fading model," *IEEE Trans. Antennas Propag.*, vol. 64, no. 8, pp. 3597–3610, Aug. 2016.

[10] V. M. Renno *et al.*, "On the generation of α-η-κ-μ samples with applications," in *Proc. IEEE 28th Annual Int. Symp. Pers., Indoor, and Mobile Radio Commun. (PIMRC'17)*, Oct. 2017, pp. 1–5.

[11] A. A. dos Anjos *et al.*, "Higher order statistics for the α-η-κ-μ fading model," *IEEE Trans. Antennas Propag.*, vol. 66, no. 6, pp. 3002–3016, Jun. 2018.

[12] H. Lei *et al.*, "Secrecy capacity analysis over α-μ fading channels," *IEEE Commun. Lett.*, vol. 21, no. 6, pp. 1445–1448, Jun. 2017.

[13] H. Lei *et al.*, "On physical layer security over generalized Gamma fading channels," *IEEE Commun. Lett.*, vol. 19, no. 7, pp. 1257–1260, Jul. 2015.

[14] H. Lei *et al.*, "On physical layer security over SIMO Generalized-K fading channels," *IEEE Trans. Veh. Technol.*, vol. 65, no. 9, pp. 7780–7785, Sep. 2016.

[15] I. S. Gradshteyn and I.M. Rhyzhik, *Table of Integrals, Series and Products*, 7th ed., A. Jeffrey and D. Zwillinger, Eds. Burlington, MA, USA: Academic Press, 2007.

[16] M. Abramowitz and I. A. Stegun, *Handbook of Mathematical Functions with Formulas, Graphs, and Mathematical Tables*, 9th ed. New York, NY, USA: Dover, 1972.

[17] A. P. Prudnikov, Y. A. Brychkov, and O. I. Marichev, *Integrals and Series*, vol. 3, New York: Gordon and Breach Science, 1990.

[18] M. D. Springer, *The Algebra of Random Variables*, New York, NY, USA: Wiley, 1979.

[19] P. K. Mittal and K. C. Gupta, "An integral involving generalized function of two variables," *Proc. Indian Acad. Sci.-Sec. A*, vol. 75, no. 3, pp. 117–123, Mar. 1972.

[20] V. S. Adamchik and O. I. Marichev, "The algorithm for calculating integrals of hypergeometric type functions and its realization in REDUCE system," in *Proc. Int. Conf. Symbolic and Algebraic Comput.*, pp. 212–224, Aug. 1990.